

TECHNICAL MEMORANDUMS
NATIONAL ADVISORY COMMITTEE FOR AERONAUTICS

No. 984

University of Maryland
Glenn L. Martin College
of Engineering and Aero-
nautical Sciences
Library

THE MECHANICAL PROPERTIES OF WOOD OF DIFFERENT MOISTURE
CONTENT WITHIN -200° to $+200^{\circ}$ C TEMPERATURE RANGE

By Franz Kollmann

VDI-Forschungsheft 403, July-August 1940

Washington
September 1941

THE UNIVERSITY OF CHICAGO

PHYSICS DEPARTMENT

1950

1951

1952

RECEIVED

PHYSICS DEPARTMENT

CHICAGO, ILL.

1953

1954

1955

NATIONAL ADVISORY COMMITTEE FOR AERONAUTICS

TECHNICAL MEMORANDUM NO. 984

THE MECHANICAL PROPERTIES OF WOOD OF DIFFERENT MOISTURE
CONTENT WITHIN -200° TO $+200^{\circ}$ C TEMPERATURE RANGE*

By Franz Kollmann

SUMMARY

The changes in the mechanical properties of wood with temperature are of importance from the biological as well as the technical point of view. Systematic experiments were therefore undertaken with special reference to the effect of gross specific weight (specific weight inclusive of pores) and the moisture content of wood. It was found that the modulus of elasticity of wood at room temperature and frozen at -8° is practically the same. At lower freezing temperatures the drop in Young's modulus with the moisture content is less than at $+20^{\circ}$. (See fig. 7.)

There is a linear relationship between the compression strength and the temperature of anhydrous wood which remains above $+160^{\circ}$. (See figs. 10 to 12.) The slope of the straight lines is directly proportional to the gross specific weight of the wood (fig. 13). In connection with these tests it was also shown that swelling of wood in liquid air does not occur; the linear heat expansion for fir between -190° and $+20^{\circ}$ was also computed.

The effect of moisture on the compression strength of frozen wood was accurately explored. The curve (fig. 17) has two peaks: one at the boundary between pure surface absorption and capillary condensation, the other at the high moisture content at which a connected "ice lattice" first begins to form in the frozen wood. Theory and experiment are in good agreement in this respect. The decrease in strength by maximum moisture content is derived from the pressure-temperature chart of ice (fig. 18).

* "Die mechanischen Eigenschaften verschieden feuchter Hölzer im Temperaturbereich von -200 bis $+200^{\circ}$ C." VDI-Forschungsheft 403, XI Bd., July-August 1940, pp. 1-18.

The compression strength of 18 species of wood was tested in relation to gross specific weight (figs. 20 to 25), which included test series for kiln-drying state, for about 10 percent moisture content and for complete water saturation and $+20^{\circ}$ and -42° temperatures. Special importance is attached to the curve of water saturated, frozen wood (fig. 25) because the phase diagram of ice itself is affected by its aspect.

The flexural strength of frozen wood was secured on several water-saturated frozen samples. It is about twice as high as the bending strength of the water-saturated wood at room temperature. According to the fracture of a frozen pine sample (fig. 29), the stress distribution is similar to that of wood at room temperature and departs considerably from Navier's rectilinear distribution.

Lastly, the impact strength of frozen laminated wood was investigated, which plainly revealed a decrease with the moisture content in the hygroscopic zone (fig. 30). A new method employing a piezoelectric indicator was developed.

INTRODUCTION

The purpose of the present study was to gain a comprehensive insight into the relationship existing between elasticity, static and dynamic strength properties under prolonged low temperatures, and varyingly wet and compact wood. The scope included the modulus of elasticity in bending, the compression strength parallel to the fiber as representative of the static strength properties and, to a limited extent, the bending strength and the ultimate impact energy as characteristic for the dynamic strength. The test series dealing with the effect of the gross specific weight included the most dissimilar kinds of wood, from especially light to heavy tropical woods, while the study of moisture content and temperature centered around domestic fir and beech. Obviously only wood without flaws and of uniform growth was employed. Beech was selected as wood with scattered pores in which free water can distribute itself much more evenly than in wood with annular pores, such as ash. Laminated beech wood, TBu 20, was employed extensively in the study.

Young's modulus and the ultimate impact strength were tested on 2 by 2 by 30 centimeter specimens. The span of 24 centimeters (between supports) conformed to the German Standard DVM 2189 in the impact bending test, but was less than 15 times the height of the specimen in the bending test and so fell outside the scope of DVM 2186. This discrepancy was accepted for the reason that Young's modulus and the breaking strength under impact could be measured on one and the same specimen. The effect of the shearing forces existing in short columns on the elastic behavior during the bending test was allowed for by a mean shear factor $\beta = 17\alpha$, in addition to the strain factor α . The compression tests were made with carefully manufactured prisms of 2 by 2 by 3 centimeters, that is, right angled with annual rings or laminations, the two cross section edges parallel as far as possible. The test specimens had the minimum dimensions permissible under the DVM 2185 standard specifications.

The most important factor of the entire undertaking was an adequate refrigerating plant. It consisted of an electrically operated automatic low-temperature refrigerator of the Alfred Teves Company, Frankfort on the Main, for temperatures from -5° to -60° . (See fig. 1.) The insert of 0.5 by 0.5 by 0.5 = 0.125 cubic meter was surrounded on all four sides by cooling coils. A thermostat kept the temperature correct to within $\pm 1^{\circ}$. Two compressors driven by two electric motors of 1.5 combined horsepower served as a refrigerating machine. Two refrigerant circuits were connected in cascade cycle, using methyl chloride as refrigerant on the high-pressure side, and propane on the low-pressure side. The ice deposit due to the moisture of the inflowing air when the refrigerator was opened was, of course, inevitable. As this appeared to introduce errors and uncertainties, especially on wood of low moisture content, all samples were enclosed in hermetically sealed cylinders or weighing bottles during the cooling. It is suspected that this lengthens the time necessary for cooling the test specimens, although no definite statement is as yet warranted. Even the use of the Fourier differential equation, which at high temperatures yields very good results (references 6 and 7), was denied for lack of proved data on the heat properties of wood at low temperatures. Therefore the temperatures were measured on the inside of a small wooden block during the cooling in the refrigerator. The curve obtained is shown in figure 2. The equalizing temperature of -38° was reached

after several hours. To be completely sure, in the subsequent tests, that the state of inertia had been actually reached and particularly that the moisture in the wood was actually completely frozen, a storage period of at least 48 hours, but frequently up to one week, was decided upon.

This would seem to have made the tests a long drawn-out affair, but it had been established in preliminary tests that only one compression sample could be tested at one time on the machine and that longer technical pause was necessary because it had been supposed from the very beginning that the frozen wood must be tested between pressure plates with likewise correspondingly low temperatures. So the 7.9 kilogram steel base plate on which the specimen rests in the crushing test, as well as the ball bearing mounted pressure plate (3.1 kg) bolted on the 10-ton Mohr-Federhaff universal testing machine were removed before each test and cooled off to the same temperature as the wood. At the beginning it was hoped that tests could be made of at least several compression specimens in a row by speeding up the test procedure, but it was found that the heat from the testing machine raised the temperature of the steel plates surprisingly fast above and below the frozen wood specimens. Figure 3 gives some insight into the temperature change on the plate below the wood. During the very first test - although it lasted only $1\frac{3}{4}$ minutes - the temperature already rose from an originally -22.3° to -5.1° . On placing the second block, cooled to exactly the same low temperature as the first, the temperature remained the same so long as no load was applied, but as soon as the pressure was applied, the heat content of the testing machine became quickly active and the temperature rose from -5.1° at the beginning to $+0.8^{\circ}$ at the end of the compression test. In the succeeding tests the temperature of both steel plates gradually approached room temperature of about 15.1° .

Now it is very instructive to plot the compression strength determined in these tests as variable of the mean temperature below the block. (See fig. 4.) The compression strength of frozen wood is intimately related to the temperature surrounding the test, and a temperature rise, small by itself, is accompanied by a considerable decrease in the compression strength. The explanation for this is that each temperature increase produces melting of the frozen water in the wood or at least favors it; that the pressure increase of itself acts in this direction is, of

course, anticipated. Lastly, the mechanical energy performed in the wood because of the compression, releases heat, and ice is returned again to its normal phases in the wood, in colloiddally bound (but nevertheless condensed in finest columns between the micelles) or free liquid water. With both processes a reduction in strength compared to the frozen state is positively associated.

In order to obviate these disturbances, the following preventative measures were taken: First, only one sample was crushed at one time between the cooled plates, after which the latter were put back in the refrigerator for no less than one hour. Next, a cooled layer of heat-resistant material - a 2.5-millimeter-thick masonite-extra-hard plate - was placed between the test specimen and the base plate, the temperature of which adapted itself more quickly to that of the machine because of its longer connection with the table; lastly, a ring of fiber protective plate of 12-centimeter outside diameter, 4-centimeter inside diameter, and 18 centimeters high - previously soaked in water and frozen - enveloped the sample during the test. In addition to that, the measurements were made by two men at accelerated speed and on a well-defined schedule. Gloves were used throughout the tests.

1. MODULUS OF ELASTICITY OF FROZEN WOOD

The modulus of elasticity was established by Zeiss dial micrometer to within 0.01-millimeter accuracy from the load-deflection diagram - the load being raised at the rate of 5 kilograms up to 40 kilograms. The rigorous validity of Hooke's law in the chosen load range is shown in figure 5. The steeper deflection curve was recorded for 24-centimeter, the flatter one for 30-centimeter span (between supports). For spans $l \geq 15 h$ (h = height of section), the shear forces exert no further effect on the elastic behavior. Here, then, the modulus of elasticity E follows the equation

$$E = \frac{0.25 P l^3}{f b h^3} \quad (\text{kg/cm}^2) \quad (1)$$

with P denoting the load (kg), l the span (30 cm), b the width of the specimen (2 cm), h its height (2 cm), and f the deflection related to P (in cm).

A laminated specimen (TBu 20), stressed parallel to the planes of the ply (fig. 5), afforded $E = 143,700 \text{ kg/cm}^2$, according to this equation.

For short, prismatic columns, that is, short spans, it is

$$E = \frac{Pl}{fbh} \left[0.25(l^2/h^2) + 5.1 \right] \quad (2)$$

according to R. Baumann (reference 2) on the previously stated assumption, that the mean shear modulus $G = \frac{1}{17} E$ is applied.

Elsewhere, the writer has proved (reference 7) that equation (2) affords an unusually good allowance for the shear stress effect in ash wood. The departure of E by a 24-centimeter span, as computed by equation (2), amounted to a mere 0.9 percent as compared to that obtained for a 30-centimeter span with equation (1). This agreement even holds for laminated wood, where the validity $\beta = 17 \alpha$ was in nowise predictable beforehand. Figure 5 shows the deflection of the same laminated piece for a 24-centimeter span. The modulus of elasticity, computed from this line with equation (2), amounted to $147,800 \text{ kg/cm}^2$. The discrepancy of +2.85 percent was therefore sufficiently small for a material such as wood.

A uniformly distributed moisture across the entire section is particularly important for the bending test. Since the highest tensile and compressive stresses occur in the neutral axis, they should not present any substantial difference in their elasticity and strength characteristics from the deeper layers. The important fact that overdrying of the outside layers when drying wood, increases the bending strength considerably when compared to that of wood of equal but at the same time of uniformly distributed moisture over the section, has been known for a long time (reference 8). Conversely, wetting of the outer layers causes a decrease in elasticity modulus and bending strength, and this fact had to be taken into account in the freezing tests. This meant the use only of such samples as had been stored for a suitable period in humidifiers and thus brought to a moisture content without gradient over the cross section. Such samples were amply available in beech plywood after 9 months' storage in humidifiers.

Of these, one sample taken from a humidifier, with a relative air moisture $\phi = 75$ percent and constant temperature of $t = 20^\circ$ (corresponding to a hygroscopic wood moisture of around 12 percent) was placed without glass bottle in the refrigerator set at -50° after the modulus of elasticity at room temperature had first been determined. Then the elasticity, after 0.5, 1.5, 2.5, and 5 hours, was recorded again on the same sample. (See fig. 6, curve b.) After about 3 hours the state of inertia was reached and the modulus of elasticity rose about 18.5 percent over the initial value. But a thin coat of ice formed on the wood as a result of the freezing of condensed water; hence the conclusion suggested itself that the rise in modulus of elasticity takes place in a different manner if, during the cooling process, the wood is protected against such occurrences. A second test, in which a new sample from the same humidifier with $\phi = 75$ percent was first tested for elasticity modulus and then placed in a hermetically sealed glass cylinder in the refrigerator, confirmed it (curve b, fig. 6). In spite of the greater inertia of the glass container, the equalization was reached after 1 hour - proof that the prolonged changes in modulus of elasticity on the first sample were, aside from the internal cooling, attributable to surface icing. The specimen was weighed on a steelyard balance after removal from the glass container. The weight remained the same for the first three hours but showed some increase after five hours - probably a result of the glass having absorbed a little moisture. This test point was therefore rejected. The rise in modulus of elasticity solely through cooling amounted to 12.2 percent at the humidity in question. The error resulting from failure to protect the specimens against moisture is around 50 percent, even by the not-especially-low moisture content of the wood itself. On further dried-out samples it would, of course, be still greater.

The subsequent tests were then made with specimens cooled in glass cylinders. All specimens stemmed from one plywood panel, hence they were of uniform material characteristics.

Even so, it was impossible to prevent scattering altogether; but in order to minimize its effect on the test data, three samples of each test series were tested at each moisture content and the results averaged. The first test series was dedicated to the determination of the modulus of elasticity of the laminated specimens with different moisture content at $+20^\circ$ room temperature (lowest curve, fig. 7).

The curve resembles that found for different kinds of solid wood (reference 6). A second test series with specimens frozen at -8° surprisingly revealed the moduli of elasticity of these specimens to be practically the same as at room temperature. The points are shown in figure 7. However, the result can be explained as follows: The modulus of elasticity of ice parallel to the frozen area is 95,000 kg/cm², and 112,000 kg/cm² at right angles to it, according to Koch (reference 9). Data regarding the type of stress and temperature are not given. Hoss' data from bending tests (reference 10) are given in table I.

Incomplete as these data are, they nevertheless manifest that the modulus of elasticity of ice can, in order of magnitude, approach that of laminated wood.

TABLE I

Modulus of Elasticity of Ice
(from bending tests, L = length, B = width, D = thickness)

Temperature	State of Test Piece	Modulus of elasticity kg/cm ²
0 to -1	Principal axis parallel to L	182,000
-2 to -5	----- do.----- L	59,000
0 to -1	----- do.----- B	383,000
-1 to -5	----- do.----- B	418,000
-1 to -5	----- do.----- D	254,000
-1 to -3	Coarse grain	285,000
0 to -3	Fine grain	226,000
Probable value for arbitrary ice (obtained in different manner by averaging)		276,000

More definite statements are out of the question, especially since nothing is known regarding the icing in the wood, that is, the plane of layer, grain size, etc. It is, of course, important that the thermal expansion factors of ice and wood are fairly close to each other, so that the ice adhering to the micelles of the wood fibers does not reduce its content more than the wood when the temperature drops. Negative pressures or tensile stresses on the micelle structure do not occur. On rocks, where the cubic expansion is one-tenth lower than on ice, such negative pressures are inevitable and interpreted as contributory cause of the weathering phenomena (reference 11).

From the foregoing bending tests at -8° , it can be rightly concluded that at this temperature the modulus of elasticity of the frozen colloidal water in the wood cannot be radically different from that of wood. Regarding the elastic behavior of wood itself at sinking temperature, nothing was known for the time being. Two test series on specimens cooled at -30° and -50° gave the curves also shown in figure 7. These curves, at 0 percent moisture, have about the same starting point but then break apart; the decrease in modulus of elasticity with the moisture content becoming less as the temperature becomes lower. Then the computation of the proportional increase in modulus of elasticity at -50° with respect to wood at room temperature, followed by coordination of these values to the relative moisture contents yields, apart from a breakaway at 13.4 percent moisture, a straight line through the point of origin (fig. 8). This proves that the comparative rise in modulus of elasticity of wood cooled to low temperature relative to wood at room temperature or at not abnormally low temperatures is solely bound up with property changes of the swelling water frozen in the wood.

From this it is concluded that the modulus of elasticity of the ice in wood below -8° becomes gradually higher than that of the wood and therefore gains in significance for the elastic strains. This significance must, according to the foregoing agreement, be so much greater as the temperature of the ice is lower and the more ice that is contained in the wood. On the elastic behavior of wood itself, the temperature drop in the questioned range has no effect or only a slight effect. This is probably explained by the fact that the elastic behavior of wood is governed by the microscopic fibers, particularly the intergrowth of the supporting fibers in deciduous wood (the tracheids in conifers). These biologically induced conditions are scarcely changed by the cooling. A simple consideration, however, dictates that pronounced temperature effects are a natural result in strength tests where the breaking stress is dependent upon the internal cohesion and hence, on given conditions of the submicroscopic structure because here the volume reduction on cooling must express itself in greater internal adhesive power. This problem is analyzed in the next section.

At the conclusion of the measurements the proportional rise of modulus of elasticity of building timber of different moisture contents at cooling from room temperature to -35° was also established (table II).

TABLE II

Modulus of Elasticity of Different Kinds of Wood
at +20° and -35°

Species	Gross specific weight g/cm ³	Moisture content u percent	Modulus of elasticity E	
			at +20° kg/cm ²	at -35° kg/cm ²
Beech	0.67	9.0	133,200	140,500
Oak*	.60	11.2	90,200	100,000
Ash	.62	9.5	116,200	128,400
Fir	.465	7.5	97,000	99,000

*Fibers run irregularly.

2. EFFECT OF TEMPERATURE ON COHESION, STRENGTH, AND HEAT EXPANSION

As the temperature rises, the resistance to form changes of every solid or liquid substance - constant in structure and composition - decreases in conformity with a general law of temperature governing the mechanical behavior of bodies (reference 12).

For metal, the proof has been adduced by comprehension tests. To illustrate: copper, magnesium, cadmium, tin manifest a steady and, to a large extent, linear decrease, while in iron and nickel - probably due to the presence of transformation points - the decrease is less uniform. No systematic studies are known for wood except for a few short articles (references 13 and 14). The loss of strength above about +120° has, of course, been stressed at times but this was always ascribed to chemical - never to physical - causes (reference 15). Since the very first compressive tests on red-beech wood disclosed that wood cooled to -50°, even in a completely anhydrous state, had a substantially higher compressive strength than wood at room temperature, the temperature effect was explored throughout the range from about -190° to +220°. The -190° temperature was produced with liquid air kept in a Dewar vessel in order to prevent evaporation of nitrogen as much as possible. But even then, a gradual enrichment of oxygen was unavoidable as found from the increasing density of the liquid air (cf. Landolt-Börnstein, 5. Aufl., Bd. I, S.277).

Technical difficulties were also involved in the task of assuring safe cooling of wood in liquid air without absorbing some of it. This problem seemed important since it was not known whether a swelling occurs in the liquid air, under which the cohesion decreases as a result of enlarged micelle distances and so acts against the temperature effect. The test pieces therefore were fused in very thin glass capsules and buried for several hours in liquid air. To assure proper heat transfer within these glass containers, copper chips around the wood acted as cold conductors. The points secured for -190° were sufficiently accurate on the straight line, which was anticipated according to the tests at somewhat higher temperatures. The scatter is, of course, greater at this low temperature than at the higher temperatures, but it might be attributed to unavoidable test errors (especially to the cooling losses). Admittedly, it is not possible theoretically, to reach higher values if the compression test itself is made in the neighborhood of -190° . The proof was adduced as follows: A compression piece was dipped direct in liquid air and cooled off in it. Previous to the test, the specimen (fir No. 31) weighed 5.163 grams, with a volume of 11.16 cm^3 ; in the liquid air it absorbed about 1.74 grams, so its weight, after the cooling, amounted to about 6.9 grams. More accurate data were impossible since, in spite of the quickest possible removal and weighing on a semi-automatic chemical balance, some liquid air evaporated and falsified the result of the weighing. However, this was not very important for the subsequent estimate and conclusions. At the cited temperature, the liquid air already consisted largely of liquid oxygen; its specific gravity was about 1.12 g/cm^3 ; that is, 1.74 grams had a volume of 1.95 cm^3 . If this liquid amount had been absorbed intermicellarly through swelling, the content of the wood sample would have had to increase by approximately

$$\frac{1.95 \times 100}{11.16} \approx 17.5 \text{ percent}$$

As a matter of fact, the immersed wood not only failed to disclose any increase in volume but on the contrary, disclosed a reduction in volume. Radially, the kiln-dried block measured 19.46 millimeters at room temperature (20°) as against 19.38 millimeters after removal from the liquid air - thus being contracted 0.41 percent. Tangentially, it measured 19.10 before testing, and 19.01 after the liquid-air treatment - a contraction amounting to 0.42 percent.

The previously cited large amount of liquid air therefore could not have penetrated the micelles, as they were not driven apart but rather brought closer together by the cooling; hence the liquid air must have been absorbed capillarily. Theoretically this is easily possible in the presence of the large proportion of pores in the employed fir wood - amounting to $1 - (0.426/1.50) = 0.716$ for a gross specific weight (with pores) of 0.426 g/cm^3 and a net specific weight (pores subtracted) of 1.50 g/cm^3 . With 12.02 cm^3 volume, the wood block could absorb $12.02 \times 0.716 \times 1.12 = 9.64$ grams of liquid air by complete filling of all cell cavities. The comparatively rapid absorption of liquid air is also comprehensible since the viscosity of liquid air (Landolt-Börnstein, 5. Aufl. Bd. I, S. 184) amounts to $\eta = 0.001858 \text{ g/cm s}$ (physical scale) at around 183.5° , while the viscosity of water at 20° ($\eta = 0.01006 \text{ g/cm s}$) is about 5.7 times as high.

These figures for the linear dimensional changes transverse to the fiber can also be applied to an appraisal of the mean coefficient of expansion between $+20^\circ$ and -185° . It is

$$l_2 = l_1 [1 + \beta_w (t_2 - t_1)] \quad (3a)$$

or

$$\beta_w = \frac{l_2 - l_1}{l_1 (t_2 - t_1)} \quad (3b)$$

Inasmuch as the contraction radially and tangentially was about equal to the annual rings, only one case need be analyzed. Radially, we get $l_2 = 19.38 \text{ mm}$, $l_1 = 19.46 \text{ mm}$, $t_2 = -190^\circ$ and $t_1 = +20^\circ$, hence

$$\beta_w = \frac{19.38 - 19.46}{19.46 \times (-190 - 20)} = 0.0000196$$

Reference 4 quotes 0.0000341 to 0.0000584 for the linear expansion of fir and pine at right angles to the fiber at ordinary temperatures. Our own observation fits into the general picture, that the expansion coefficients of solid bodies increase, as a rule, with rising temperature. The theoretical connections, admittedly, are very complicated for anisotropic bodies. For nonregular crystals (wood may be figured to the rhombic crystal system in elastic behavior), the expansion coefficients depend primarily upon the size of the elasticity moduli - in the

sense of Voigt's crystal physics in the principal directions - and on the thermic pressure coefficients and their changeability with temperature. The latter are approximately proportional to simple Debye atomic heat functions (reference 16). Some very unusual phenomena can occur through alternations of the effects.

An intermediate point between the liquid air temperature and the lowest temperature attainable in the refrigerator was established by means of dry ice (-82°). Temperatures above $+20^{\circ}$ were produced in a thermostatically controlled Heraeus drier. The plotting of all test points for completely anhydrous fir wood afforded a rectilinear relationship (fig. 9) between compressive strength σ and temperature t , which can be expressed by

$$\sigma_2 = \sigma_1 - n (t_2 - t_1) \quad (4a)$$

or, for $t_1 = 0$ and $t_2 = t$:

$$\sigma_t = \sigma_0 - n t \quad (4b)$$

Therefore, figure 9 discloses, for example, $\sigma_t = 1050$ kg/cm² for $t = -100^{\circ}$ and $\sigma_0 = 850$ kg/cm² for $t_1 = \pm 0^{\circ}$; hence, $n = 2$ for the above equation. Accordingly, it affords $\sigma_t = 850 - (2 \times 220) = 410$ kg/cm² for $t = +220^{\circ}$. This strength is exactly the same as obtained in the tests.

Since it is not feasible to draw general conclusions from tests on one species of conifer, further measurements of the temperature effect on the compressive strength were carried on with kiln-dried and air-dried red beech, laminated beech, and balsa wood (figs. 10 and 11). It was found that, without exception, a rectilinear temperature-compressive strength relationship exists, that at above $+160^{\circ}$ a more-than-proportional drop takes place (laminated wood is inferior to solid wood in this respect), that the scatter of the test values is greatest at the lowest temperatures, and that the proportional strength decrease increases with increasing gross specific weight r_0 of the wood. The last-cited fact becomes particularly plain if all curves are combined in one graph (fig. 12). The pitch of the straight lines is so much steeper as the specific weight of wood is higher. Thus, when the test values for n ($= \tan \alpha$ in an equally divided net) are computed from

equation (4b) and the corresponding figures from figure 12, it is found that n is directly proportional to the gross specific weight r_0 of the wood (fig. 13). The scatter itself is surprisingly small. It is

$$n = 4.76 r_0 \quad (5)$$

which, written in equation (4b), gives

$$\sigma_t = \sigma_0 - 4.76 r_0 t \quad (4c)$$

The constant 4.76 has the dimension (cm/°C), which is readily secured.

Lastly, it remained to be proved at what upper temperatures - and, if necessary, after what interaction in time rate of these temperatures - the reversible physical temperature effect is accompanied or exceeded by a nonreversible chemical disintegration. Chemical changes in wood are, in general, according to literature, said to occur above 120°, although the chemical decomposition of any appreciable speed does not occur below 250° (reference 17). Only Marschallek (reference 18) pointed out that a temperature of +160° results in a slight increase in compressive strength rather than a decrease.

For our own experiments, prisms of usual sizes for compression tests were machined from fir, red beech, and plywood - kiln-dried at 100° and tested after cooling; other prisms were heated for one, two, and four hours each, at 160° and 200° in the drier, followed by cooling to room temperature in the desiccator over phosphorus (P_2O_5), and crushed. The results (figs. 14 to 16) clearly show that a temperature of 160° causes no change whatever in compressive strength of fir or beech. On laminated wood the synthetic resin content, of course, resulted in a slight loss of about 3 percent after four hours at 160°. At 200° a disintegration of the wood constituents is inevitable after a prolonged period, as evidenced by a marked brownness of the wood.

3. COMPRESSIVE STRENGTH OF FROZEN WOOD

a) Effect of Moisture Content

For the tests, a specially uniform growth of red beech

with a mean gross specific weight of 0.696 g/cm^3 , kiln-dried, was available. Specimens for the compression tests in the hygroscopic zone were cut to 2 by 2 by 3 cm from pieces directly out of the humidifier. Damp wood, that is, wood with a content of free water, was obtained by soaking the blocks in water prepared in a vessel under negative pressure. To produce the changes due to freezing, the specimens of the first test series were crushed at room temperature. The rate of loading was intentionally chosen higher than the DIN standard DVM 2185 because on the subsequent frozen specimens the shortest possible compression process is essential. In this connection it may be stated that the specified DIN standard DVM 2185 of 200 to 300 kg/cm^2 min as rate of loading is a little low. This is equally evident in the specifications for airplanes and gliders (ed. December 1939), which give 400 kg/cm^2 min for ash and pine, 350 kg/cm^2 min for linden and all other conifers, and 800 kg/cm^2 min for laminated wood in compressive tests. To be sure, the specifications state that the rate of loading per minute should not exceed the compressive strength in kg/cm^2 of the particular wood. Since the breaking strength of unfrozen wood drops to around 300 kg/cm^2 with the moisture content, compliance with the latter requirement of the design specifications for aircraft would dictate the upper load rating of the 2185 standard.

For the frozen wood - with compressive strength as high as 1400 kg/cm^2 , according to the tests - this would entail a test period of from 4 to 5 minutes, and that would have been too long in spite of all preventative measures against inadmissible heating. Furthermore, the marked plasticity of ice near the zero point (references 19 and 20) may cause errors in measurements if the tests are prolonged. Since the compressive strength of frozen wood is very high, the rate of loading can be raised without infringing upon the aircraft-design specifications. A timing of the loading rate to fit the occasionally supposed compressive strength is, on the other hand, impossible for various reasons. Hence, a constant test speed of around 800 kg/cm^2 min was decided upon. This probably involves a slight increase in compressive strength (references 21 and 22), but the rise should be fairly equivalent in proportion on the specimens of various moisture contents and different cooling.

The compression test data on beech with different moisture content at room temperature and after freezing at -42° are given in figure 17. The curve for the wood at

normal temperatures has a completely normal aspect. The strength decrease of red beech is almost linear. Other woods also manifest this fact, while for still other species - such as fir - the curve is convex in the region of little moisture content, up to the kiln-dried state.

The equation for the relation of compressive strength of beech at room temperature, with moisture u within range of 0 to 20 percent, reads:

$$\sigma_2 = \sigma_1 - n (u_2 - u_1) \quad (5)$$

Putting $\sigma_2 = 450 \text{ kg/cm}^2$ for $u_1 = 20$ percent and $\sigma_1 = 1100 \text{ kg/cm}^2$ for $u = 0$ percent, affords $n = 32.5$; that is, the compressive strength of red beech decreases per 1 percent moisture-content increase by 32.5 kg/cm^2 , and vice versa. This absolute estimate is substantially more accurate than the usual conversion in the testing of materials (cf. DIN DVM 2185), where a 5-percent decrease or increase in the compressive strength of wood per 1 percent moisture increase or decrease serves as a basis. This method is useful only in a very narrow range of moisture content. In the kiln-dried state and for very low moisture contents, the proportional change in compressive strength is substantially less than 5 percent per 1 percent of moisture variation. In our case, for instance, a moisture rise from 0 to 1 percent afforded a decrease of $0.05 \times 1100 = 55 \text{ kg/cm}^2$, while as proved in the foregoing, only 32.5 kg/cm^2 should really be subtracted. The error amounts to nearly +70 percent. Between 19 and 20 percent, on the other hand, the empirical formula would give $0.05 \times 482.5 = 24.2 \text{ kg/cm}^2$; or the considerable error of around 25 percent, even though it acts in the opposite sense. A completely exact 5-percent increase or decrease per 1 percent of moisture change is afforded only by a moisture, at the beginning of which a 5-percent strength change per 1-percent moisture change amounts to 32.5 kg/cm^2 . This happens from 650 kg/cm^2 on; that is, by about 13 percent moisture content.

The compressive strength of the frozen prisms is shown in figure 17. The kiln-dried wood has a much greater strength at low temperatures than at room temperature. The next test on a prism with 3.62 percent moisture content revealed an even higher compressive strength; then a uniform decrease, the curve running approximately parallel to that for room temperature. This parallelism continued even be-

yond the fiber-saturation region - that is, in the presence of free, liquid water up to about 40 percent moisture content. Then the strength increased again, to be followed by a second decrease at maximum-moisture content in the vicinity of the saturation point of the wood.

In spite of the unusual aspect of the curve, it can be physically explained and brought in accord with other observations. The necessity of the different starting point has been pointed out before. Since there is no water in the wood and a change of state of aggregation of other chemical constituents at the temperature in question is excluded, the difference cannot be other than physical. This is dictated by the general temperature law for solid bodies and traces back to a lattice change as a result of the temperature drop. The amount of strength discrepancy is, as already stated, proportional to the temperature difference. With equation (4c) we get for -42° from the strength of red beech, with $r_0 = 0.696 \text{ g/cm}^3$ at $+20^{\circ}$ in height of $\sigma = 1100 \text{ kg/cm}^2$, a "cold strength" of

$$\sigma_{-42} = 1100 - 4.76 \times 0.696 (-42 - 20) \approx 1305 \text{ kg/cm}^2$$

as against 1355 kg/cm^2 actually observed.

The first small quantities of hygroscopic moisture are avidly absorbed by the cellulose frame of the wood by virtue of the powerfully active surface forces and are precipitated on the inner surface. This absorption continues until the inner surface is covered with a layer of water of molecular thickness. If the swelling, that is, the absorption of colloidal water in the wood continues, the surface absorption changes to capillary condensation, where the interspaces between the cellulose micelles fill with submicroscopic fluid columns. The boundary can be mathematically defined as follows: The limiting moisture u is

$$u = O c \delta (\gamma_F / \gamma_H) 100 \text{ (percent)} \quad (6)$$

where O is the inner surface ($\text{cm}^2 / 1 \text{ cm}^3$ cellulose), c the cellulose portion of the wood, δ the thickness of the molecule of the absorbed fluid (cm), γ_F the specific weight of absorbed fluid (g/cm^3) and γ_H the net specific weight of the cellulose. This approximates (reference 6) $O = 6 \times 10^6$ to 10×10^6 ($\text{cm}^2 / \text{cm}^3$), $c = 0.67$ (for red beech, according to C. G. Schwalbe and E. Becker). $\delta = 9 \times 10^{-9}$ (cm)

(according to Landolt-Börnstein), $\gamma_F = 1.0$ (g/cm³) for water, and $\gamma_H = 1.50$ (g/cm³).

With these figures, we get:

$$u = 6 \times 10^6 \text{ to } 10 \times 10^6 \left(0.67 \times 9 \times 10^{-9} \times \frac{1}{1.5} \right) \times 100$$

$$= (0.024 \text{ to } 0.040) \times 100$$

The extreme moisture content at which minimum water columns form between the micelles, therefore, ranges from 2.4 to 4.0 percent, averaging 3.2 percent for beech wood.

Above $+0^\circ$ the surface absorption of water stipulates a decrease of strength at the cellulose micelles because the micelle distances become greater; hence the mutual adhesive powers of the micelles which, in turn, bring about the cohesion, become less. But below $+0^\circ$, this process is counteracted by stiffening of the micelle bond due to the icing. That break phenomena are initiated on bodies with cellulose frame by micelle slippage is common knowledge (references 23 and 24). Icing acts against this slippage, and if the analysis proceeds from the kiln-dried state, this effect will be so much greater as the stiffening ice film of the inner surface of the wood becomes denser. A limiting value must positively be reached at the point where the entire inner surface is precisely covered with a continuous, but the thinnest possible ice film. This point corresponds to the previously estimated moisture limit between surface absorption and capillary condensation. Further accretion of ice will not enhance the cohesion because ice itself has a very low specific strength. On the contrary, the strength then decreases, corresponding to the increased micelle spacing as a result of the progressive swelling. The adhesive forces exerted by the micelles on each other depend solely on their spacing, regardless of whether these are increased by interspaced fluid water or ice. Strictly speaking, the rate of increase in spacing on changing from water to ice should, of course, raise a little at a certain moisture content because the specific volume of ice exceeds that of water. But the effect is so slight that it cannot be proved in the test. It is obvious that this parallelism of moisture and strength curves of wood at room temperature and frozen, must positively continue as far as the fiber saturation region. Below this region, that is, on admittance of free liquid water in the coarser capillaries, the strength no longer changes

for temperatures above freezing point, since the swelling processes are terminated.

But if the capillary water turns to ice, the effect can be very dissimilar, depending upon the moisture content. In the first region - that is, up to about 40 percent - the curves for frozen and unfrozen wood are still parallel; the rising ice content affects the strength no more than the rising content of fluid water. Further saturation gradually fills coarser capillaries completely with water. Then, if these replete cells congeal, their strength must positively rise, as that of a hose which, filled with water, can practically take up no crushing pressure but is well able to do so if its contents are frozen. Above 40% moisture content the compressive strength of the frozen wood thus rises again gradually, and approximately reaches the compressive strength of the unfrozen wood, with only 15 percent moisture content. Now it could be imagined that this strength rise continues so long as the content of capillary water increases; this would be up to the highest possible moisture content u_{max} , which depends upon the volume of the pores:

$$u_{max} = u_{FSP} + \frac{\gamma_H - r_0}{\gamma_H r_0} \gamma_W \quad (7)$$

where u_{FSP}^* is the wood moisture content at fiber saturation point (= 0.28 for the explored red beech), γ_H the net specific weight of the wood (= 1.50 g/cm³), γ_W the specific weight of capillary water (= 1.0 g/cm³), and r_0 the gross specific weight of the wood in the kiln-dried state (= 0.696 g/cm³, in our example).

Hence we get for the explored wood,

$$u_{max} = 0.28 + \frac{0.804}{1.50 \times 0.696} = 1.05$$

But considerably below this moisture content, a point where a kind of coherent ice lattice begins to form is already reached. The process is somewhat as follows: When the cells, averaging 31 percent in red-beech wood (reference 25), are completely filled with ice, such a lattice occurs; that is, connected ice filaments pervade the entire

*FSP = fiber saturation point.

volume of the wood, hence reach from pressure plate to pressure plate and thus actively participate in the force transfer. On the particular red-beech wood it defines a moisture content of about

$$u_{\text{FSP}} + \frac{\text{cell portion}}{r_0} = 0.28 + \frac{0.31}{0.696} \approx 0.83$$

At 83 percent moisture content the ice lattice in the explored red beech therefore participates in the transfer of the pressure and, being less plastic than the unusually deformable wood at such high moisture, it is more strongly attracted than the wood - hence high pressures are exerted on the ice. These can also be estimated when referring the maximum compressive stress reached at the particular point, to the surface portion of the ice at the cross section of the wood (that is, the cell portion). We get (see the test point at $u = 0.86$ in fig. 17) $\frac{980}{0.31} \approx 3160 \text{ kg/cm}^2$. But the ice in the wood starts to melt at a much lower pressure. This is explained as follows: The capillary water in the wood was frozen at normal-atmosphere pressure, hence ice modification I was formed. The equilibrium curve between this anisotropic crystal phase and the isotropic fluid phase in the pressure-temperature chart, according to Tammann (reference 26) and Bridgman (reference 27) is shown in figure 18. The melting point is seen to be so much lower as the pressure is higher; for 2200 kg/cm^2 , it lies at around -22° . But our own tests have proved that the temperature of the compression specimens rises during the compression test. To illustrate: In figure 3, the mean temperature under a block during the first test - i.e., with freshly cooled plates, amounted to about -14° ; but a 1500 kg/cm^2 pressure is enough to make ice I melt at this temperature.

From all these facts, it is concluded that the above-described formation of a coherent ice lattice in the wood must lead to melting of the ice during the compressive stress. The consequence of this melting is a drop in the compressive strength, as reflected on the curve in figure 17, for the frozen wood. The drop occurs at a moisture content of about 85 percent. Theory and test data are thus in good agreement. The physically unusual relationship between compressive strength of frozen wood and phase diagram of the ice is discussed elsewhere. The freezing-point decrease associated with the pressure rise also

stands out because of the sudden appearance of liquid water despite the low temperatures. The process during the stress is as follows: At first the ice lattice takes up the principal stress; in spite of the low compressive strength of the ice itself, it is possible because the lattice is solidly imbedded in the wood mass. The compressibility of ice (reference 9) at low pressure is $\kappa = 1.2 \times 10^{-5}$ cm²/kg; but, according to the discussed connections between pressure and melting point of ice I, the latter liquifies on exceeding a corresponding temperature. Then the wood with its low strength and great plasticity, as a result of the maximum micelle spacing due to swelling, and of the suppression of the reinforcing effect of the ice (since it melts), can again be made to share in the support. The deformation of the wood therefore proceeds very rapidly and after a comparatively small compression, a still undamaged, unmelted piece of the ice later comes into action again. This play is repeated in all its details, and the result must be a decrease in compressive strength.

This brings us to the rise in compressive strength due to cooling and freezing from the technical and physiological point of view. The proportional increase itself is very informative (fig. 19). The curve plotted from the test data has two hyperbolically ascending branches up to the fiber saturation point; a point of discontinuity lies at the previously discussed extreme moisture content, where the surface absorption at the cellulose micelles is ended. Above this saturation point, the curve of the proportional strength increase is similar to that of the compressive strength of the frozen wood. Since the compressive strength of wood at a temperature above 0° remains constant in this zone, the proportional strength increase must be proportional to the strength itself. It should be remembered that, according to earlier experiences, the strength increase was not associated with ice formation but with a temperature drop. General data about a certain strength increase of frozen wood without consideration of the temperature are therefore just as worthless - yes, defective - as the tests in which moisture content and gross specific weight of the wood had not been accurately determined. The -42° freezing temperature, on which the tests illustrated in figure 17 have been based, lies in the neighborhood of the lowest temperatures to which wood in a living tree is exposed. It also should be a significant temperature for wooden parts of buildings and aircraft. At slightly lower temperature, the temperature of-

fect is less - hence the strength increase is lower. Thus, the proportional strength increases plotted in figure 19 may be considered as upper-limit values, whereby the moisture contents anticipated in the mean under different circumstances must be kept in mind. On airplane parts it should range from 13 to 15 percent. The compressive strength increase in this zone amounts to about 60 to 67 percent. On wood used for antenna towers, scaffolding, platforms for ski jumping, centering, bridges, etc., the strength increases range from 80 to 120 percent. This applies, of course, to red beech only; other species of wood have different gross specific weights and must be treated accordingly, as explained farther on. Red-beech trunks, in the forest, have an average moisture content of 65 percent; freezing of this water content at the quoted temperature results in a compressive-strength increase of about 180 percent. From the biological angle, the compressive strength is not as important, of course, as the elasticity modulus, for a tree loaded down with snow is usually stressed in buckling, that is, the first Euler case is involved; one end (root stock) being restrained, the other (treetop) free. Discounting in first approximation the variable inertia moment of the trunk, the buckling load is proportional to the elasticity modulus. (Cf. table II.) Moreover, freezing of the entire cross section is likely to be very rare. During the unusually severe winter of 1939-40, the author observed freshly felled pine trunks of from 30- to 40-centimeter diameter in Upper Bavaria, with up to 6-centimeter (only) ice coatings in the center zones.

b) Effect of Gross Specific Weight

The different gross specific weights of kiln-dried wood depend, as previously pointed out, solely on the pore proportion c , since the net specific weight of the cell-wall substance of all wood is the same - whether deciduous or coniferous, and irrespective of habitat. Thus, from the theoretical point of view, the compressive strength σ_0 of wood with specific gross weight r_0 must be obtainable from the compressive strength $\sigma_0 \gamma$ of a poreless wood prism with net specific weight $\gamma = 1.50 \text{ g/cm}^3$:

$$\sigma_0 = (1 - c) \sigma_0 \gamma = \sigma_0 \gamma r_0 / \gamma = I_0 r_0 \quad (8)$$

The compressive strength is therefore exactly proportional to the gross specific weight. In practice, this holds

true only approximately, due to disturbing influences such as chemical constituents which, while raising the specific weight, do not increase the strength (for instance, resins) or to influences promoting compressive strength (i.e., comparatively high lignin content) (reference 28), or other anatomic peculiarities. The latter act chiefly on the shearing strength which, in the unidirectional stress condition, is - aside from the compressive strength - of great importance for the break formation. Figure 20 reproduces the relation of a number of kiln-dried woods at room temperature, along with the scatter in consideration of the very dissimilar test material. The following species were represented:

Balsa	$r_0 = 0.092$ to 0.139 g/cm ³
Umbrella tree	$r_0 = .176$ to $.182$ g/cm ³
Albizzia	$r_0 = .215$ to $.217$ g/cm ³
Fir	$r_0 = .388$ to $.427$ g/cm ³
Alder	$r_0 = .440$ to $.472$ g/cm ³
Poplar	$r_0 = .443$ to $.458$ g/cm ³
Willow	$r_0 = .443$ to $.467$ g/cm ³
Pine	$r_0 = .458$ to $.490$ g/cm ³
Limba	$r_0 = .482$ to $.525$ g/cm ³
Maple	$r_0 = .517$ to $.534$ g/cm ³
Walnut	$r_0 = .534$ to $.560$ g/cm ³
Ash	$r_0 = .550$ to $.61$ g/cm ³
Oak	$r_0 = .636$ to $.751$ g/cm ³
Red beech	$r_0 = .679$ to $.702$ g/cm ³
White beech	$r_0 = .775$ to $.810$ g/cm ³
Boxwood	$r_0 = .864$ to $.889$ g/cm ³
Lignum vitae	$r_0 = 1.268$ to 1.269 g/cm ³
Lignostone	$r_0 = 1.322$ to 1.460 g/cm ³

The test points were equalized by a straight line conformable to the method of least squares of error. With r_0 expressed in g/cm³, it gave for kiln-dried wood at $t = +20^\circ$,

$$\sigma_0 = 1640 r_0 \text{ (kg/cm}^2\text{)} \quad (9)$$

Putting $r_0 = 1.50$ g/cm³, we get $\sigma_0 = 2430$ kg/cm²; that is, the compressive strength of an ideal wood without pores. This figure is closely approached by lignostone, according to figure 20.

Next, the enumerated kinds of wood were tested in compression at room temperature (three pieces of each in every test series) at approximately 10 percent moisture content and water-saturated. The maximum moisture in the water-saturated state was computed first according to equation (7), and then reproduced as accurately as possible by repeated soaking by low-pressure method on a Pfeiffer high-power vacuum pump. The results are shown in figures 21 and 22. Incidentally, we point beforehand to the parabola $u_{\max} = f(r_0)$ in figure 25. The highest moisture contents resulting from the repeated soaking are, as a rule, very close to the theoretical limit value; only a few, such as walnut, white beech, boxwood and, particularly, lignostone, which is manufactured from red beech under high-pressure pressing, had more or less inferior water content. From the measurements, the following relations between compressive strength and gross weight were evolved:

$$\text{At } t=20^{\circ} \left\{ \begin{array}{l} \sigma_{dB} = 1076 r_{10} \quad (10) \\ \sigma_{dB} u_{\max} = 442 r_{u_{\max}} \quad (11) \end{array} \right.$$

(the points for lignostone discounted)

These simple equations are not to be considered mere empirical functions; the constant $I_u = \sigma_{dB_u} / r_u$ computable therefrom has, rather, a very plausible physical reason. The factor originally introduced by Monnin (reference 29) and since then having become an indispensable characteristic for the static strength properties of a material relative to light design, is explained as a column of the particular material and the exact length to produce crushing under its own weight. The comparison with Reuleux's conceived tearing length, the ratio of tensile strength to gross weight, which is an informative figure of merit for fibers and wires, suggests itself. The "static figure of merit," $I_u = \sigma_{dB_u} / r_u$, where dimensional equality must be observed and absence of buckling stress is, of course, tacitly assumed, is logically termed the "flattening length." It affords values in kilometers if the numerical value of the fraction is divided by 100. The profound relation of these values with the moisture content is obvious. The solidification through freezing also can be plainly explored.

On cooling to -42° , the cohesion increases and the compressive strength rises. Figures 23 and 24 illustrate the test points for wood with $u = 0$ and $u = 10$ percent along with the equalizing straight lines, the equations of which read:

$$\text{At } t = -42^{\circ} \left\{ \begin{array}{l} \sigma_{dB_0} = 1946 r_0 \quad (12) \\ \sigma_{dB_{10}} = 1558 r_{10} \quad (13) \end{array} \right.$$

In this connection equation (4c), which expresses the relation of compressive strength to temperature, is indicated. Combining this equation with equation (8) gives:

$$\sigma_t = (100 I_0 - 4.76 t) r_0 \quad (14)$$

where I_0 is the static quality factor (km), t the temperature ($^{\circ}\text{C}$), and r_0 the gross weight per g/cm^3 in the kiln-dried state. The relation shows the extent of change of the crushing length under the effect of the temperature, increasing on cooling below 0° and decreasing on heating above 0° , which brings out the relaxation and the increase of cohesion very clearly. The introduction of the value from equation (9) for I_0 suggests itself. It then affords an equation for appraising the compressive strength at any temperature and any gross weight in the kiln-dried state. But in view (cf. fig. 20) of the appreciable scattering in connection with compressive strength and gross weight on various woods, equation (14) with $I_0 = 16.40$ kilometers is suitable for very rough appraisals only. Computing the compressive strength of a wood of known gross weight and securing it by test may disclose a difference of as much as 20 percent. On the other hand, it is repeated that the errors introduced by converting the strength from one temperature to another with the aid of the discussed relation, are small.

In the unfrozen state the compressive strength of water-saturated wood is practically equal to the lowest possible compressive strength obtained on exceeding the maximum swelling value. Therefore, for the compressive strength as such, it is immaterial whether the highest possible moisture is reached or the water content is lower, provided it stays on the other side of the maximum swelling value. But in frozen wood, the conditions are entirely

different. Then the frozen capillary water has a direct strength-increasing effect because it lines and stiffens the cell cavities. Special care was therefore taken on the pertinent tests to assure the best possible u_{max} . All the test points are plotted in figure 25. The following explanation is appended:

The equalizing curve does not start at zero point but at the compressive strength of ice which, as an extreme case of strength, must be reached by a wood becoming continuously lighter with a 100-percent pore proportion. Since the numerical data for the strength of ice is so scattered in literature and not standardized, they are shown compiled in table III.

The scatter of the strength values is seen to be very substantial (the test procedure certainly has a pronounced effect); a probable value for the compressive strength of ice is 45 kg/cm^2 . Balsa was the lightest wood investigated. With a gross weight of 0.075 g/cm^3 in the kiln-dried state, it consists of 95 percent air and 5 percent cell-wall substance. For each kilogram of solid matter, it absorbs by complete saturation from 13 to 13.5 kilograms of water (≈ 1300 percent; see u_{max} in fig. 25). On the strength of this it might be assumed that the compression strength of such wood could not be radically different from that of pure ice. But as a matter of fact, it is about ten times as high. This is attributable to the specially beneficial interaction between the wood structure and the ice. Presumably, the ice - which, as a result of the employed impregnation method was, moreover, completely free of air - has a much higher compressive strength than in the ordinary state, since it is enclosed between the cell spaces of the wood. Since these cell walls have a comparatively very high tearing strength, they certainly lower the compressibility of the ice. Examination of the other test points obtained for woods with progressively increasing gross weight and hence decreasing u_{max} permits some pertinent observations up to about 0.5 g/cm^3 gross weight in the kiln-dried state. Above this weight the strength values drop abruptly. Its first occurrence was ascribed to chance or to an error in measurement, and attempts were made to prevent a repetition by check tests. But the jump not only persisted but became even more plain as the number of test values increased. So the first-obtained curve for the very light and the light species of wood breaks off suddenly and the strength of the more compact wood appears in a curve of lower location.

TABLE III

Strength of Ice

Type of ice and stress	Compressive strength		Tensile strength		Source
	kg/cm ²	at t ^o	kg/cm ²	at t ^o	
Parallel To at right natural angles Surface	75 130	-11	70 to 175	-7	Hütte: Des Ingenieurs Taschenbuch, 26. Aufl. Berlin. W. Ernst & Sohn, 1936, S. 890.
Test piece of distilled water or of finely powdered ice with distilled water	34.0 to 42 to 54.4	-8	14.8 to 17.0 to 24.8	-8	Romanovicz, H., and Honigmann, E. J. M. Zug- und Druckfes- tigkeit von Eis - Forsch. Ing.-Wes., Bd. 3 (1932), S. 90.
Ice of water- soaked snow	34	-3.5	7.6 to 12.7 to 19.1	-3.5	Haefeli, R., 1939 (19)*
Ice of non- distilled water	--	--	2.6 to 5.7 to 11.2	-3.5	
Natural icicles	--	--	9.5 to 12.5 to 19.0	-3.5	
Milky ice	40 to 80	-5 to -9	50 to 120	-5 to -9	Bautechnisches Labora- torium der T. H. Munche (briefliche Mitteilung)
Clear ice	30 to 100				

* Reference 19.

On the basis of the cited phase diagram for ice, an explanation for this peculiar behavior is indicated. The "ice lattice" in the wood is so much more compact and has so much greater total cross section as the weight of the wood is lighter - that is, the more water per unit volume it contains when completely saturated. And since at the same time the highest loads are comparatively small, the lightest woods in ice show compressive stresses of from 600 to 800 kg/cm². As the gross weight rises, the ice portion becomes less, hence the ice lattice becomes continuously finer. Then, when it is observed that it results in steadily rising stresses, it may be assumed that it contributes substantially toward the absorption of the pressure. By a gross weight in the kiln-dried state of around 0.5 g/cm³, stresses of at least 1000 kg/cm² are reached. For beech wood with $r_0 = 0.696$ g/cm³, a theoretical compressive stress in ice of more than 3000 kg/cm² had been computed earlier in the report. Now to each pressure (fig. 18) a melting point can be coordinated which is located as much lower as the pressure is higher. To illustrate: For 1000 kg/cm² the melting point defines -9° , for 1500 kg/cm², about -14° . It was stated elsewhere that the mean temperature under the test pieces in the compression test is higher than the freezing temperature of the wood in the refrigerator (fig. 3). By reason of the combined action of all of these factors, a limit evolves which, with the chosen test procedure and temperature ranges for the present at $r_0 = 0.5$ g/cm³, a limit at which the compressive stresses in the ice are sufficient to bring it to melting. This naturally is accompanied by an immediate decrease in the breaking stresses of the frozen wood, since the surrounding wood is softened again by the melting water. This fully explains the discontinuous aspect of the curve, but it remains to prove the theory by an actual test. This was accomplished as follows: The melting point depends upon the pressure and temperature, so if care is taken to keep the temperature of the pressure plates especially low and preclude any cold losses, the melting starts at higher pressures than it would without these precautionary measures. With this in mind, several tests were made between pressure plates cooled in dry ice; as anticipated, the test points - indicated thus: 6 (fig. 25) - fell on the continuation of the first curve. The break was gone. In practice, of course, such low temperatures can be reckoned with only in very rare cases. Ordinary freezing temperatures are not sufficient for protecting frozen wood containing much water under compression.

from melting of ice in the wood under increasing stress and hence against loss of strength. The problem of defining the end point in which the curve for water-saturated wood must terminate by $r_0 = 1.50 \text{ g/cm}^3$ was also explored. This was necessary because the measurements on lignostone (with $r_0 = 1.35 \text{ g/cm}^3$) gave entirely wrong figures.

The reason for this (see fig. 25) was the impossibility to bring this wood, even approximately, to a saturation moisture commensurate with its volume of pores and its mass. Since the moisture was much below the maximum swelling value, even the strength, naturally, was much too high. An ideal wood with $r_0 = 1.50 \text{ g/cm}^3$ would contain no microscopic pores, hence could absorb no free water, but merely swell colloiddally. In this extreme case, $u_{\max} = u_{\text{FSP}}$ (FSP = fiber saturation point). This holds for the frozen as well as for the unfrozen state. A compressive strength of $\sigma_{u_{\max}} = 665 \text{ kg/cm}^2$ was then extrapolated for a water-saturated wood with $r_0 = 1.50 \text{ g/cm}^3$ (fig. 22) at room temperature. According to figure 17, the compressive strength of frozen beech on the fiber saturation point in relation to nonfrozen beech is as 2:1 at the chosen test temperatures ($+20^\circ$ and -42°). This, then, affords a theoretical end point of around 1330 kg/cm^2 . Connecting this point with the zero point of the axes system, the line (-.- in fig. 25) illustrates the connection between the compressive strength and the kiln-dry weight of wood frozen at -42° at the maximum swelling value. The departure of the ordinates of the curves for water-saturated wood from the straight line of maximum swelling value gives an indication of the effect of the frozen free water on the compressive strength.

It is misleading to assume that the solidification of ice is in all cases accompanied by a greater brittleness (reference 5). If by brittleness is meant the tendency of a body to abrupt breaking under the effect of outside forces, without prior major form changes, the brittleness of ice depends to a comparatively great extent on the type and rate of stress as well as on the temperature (reference 20). On the compound body, wood-ice, the conditions are even more complicated, although the illustrated cases of failure of frozen water-saturated specimens indicate that - at the chosen test conditions - the tenacity and plastic deformability rather than the brittleness, increase. Figure 26 shows several crushed balsa pieces. While this

kind of wood when unfrozen, because of its particular anatomical structure is almost instantaneously crushed flat on exceeding the breaking strength, or splintered by sufficient low moisture (i.e., kiln-dried), the same balsa wood water-saturated and frozen manifests the usual slippage planes below 45° - that is, in the direction of the maximum shearing stresses. Denser wood, such as walnut or red beech (fig. 27), deform in the compression test, with the characteristic bulging and flattening of tenacious materials (such as brass).

4. THE BENDING STRENGTH OF FROZEN WOOD

Several pieces, used previously in the determination of Young's modulus for air dryness at room temperature and -35° , were saturated with water as far as possible by vacuum drying. A moisture content of 93 percent was obtained for beech, 99 percent for ash, but of only 55 percent for pine. This, of course, is due to the anatomic nature - that is, the presence of cells in the cited deciduous trees, and the structure of closed tracheids in coniferous wood. The water-saturated samples were then frozen at -35° and the Young's modulus secured. It amounted to $132,700 \text{ kg/cm}^2$ for beech, $113,000 \text{ kg/cm}^2$ for oak (this piece was subsequently rejected because of its crooked fibers, shown up at failure), $127,800 \text{ kg/cm}^2$ for ash, and $97,200 \text{ kg/cm}^2$ for pine. On comparing these figures with the values of table II, it is seen that the pieces which in water content are far above the fiber saturation point, regain the same stiffness by freezing that they possess in the air-dried state at room temperature. Only oak showed a substantial improvement over this state; here the ice, with its comparatively much higher elasticity modulus (table I), is more effective.

The subsequent bending tests afforded $\sigma_{bB} = 1314 \text{ kg/cm}^2$ for beech, 1080 kg/cm^2 for oak, 1366 kg/cm^2 for ash, and 960 kg/cm^2 for pine. These figures are about twice as high as the bending strength σ_{bB} of identical and equivalent water-saturated wood at room temperature. Of course, this argument must be applied with care, since the moisture content has no effect on the bending strength of unfrozen wood above the fiber saturation point, but a decided effect on the strength of frozen wood. A relationship similar to that for the compressive strength (fig. 17) might be

assumed. Then the uniform moisture distribution, so difficult to achieve in a test, is of prime importance, as manifested by Vorreiter (reference 5), who established the following stages of bending strength with the moisture content, or better, with the ice content. For fir, frozen at -14° , as follows:

Ice content	percent	22	163	196	212
Bending strength	kg/cm ²	500	580	720	770

Thunell's experiments (reference 30) on Swedish pine ($u = 12$ percent, $r_u = 0.42$ g/cm³) gave an increase in bending strength of from 760 kg/cm² at $+22^{\circ}$ to 1033 kg/cm² at -18° C, or +35.5 percent.

The texture of the break in the frozen bending specimens is fundamentally the same as in the unfrozen ones. The compression zone, in particular, discloses no appreciable difference. But in the tension zone, the room-heated wood with loose fibers and fine splinters breaks, while the frozen specimens manifest substantially more compact wedge- or even plate-like fractures. The break is accompanied almost instantaneously by a loud noise (fig. 28). Unusual also is the break on the frozen-pine specimen (fig. 29), with perfectly smooth break of the fibers in tension. On the particular pine sample, the distance of the neutral fiber from the tensed neutral axis amounted to about 6 millimeters (= 32.5 percent of specimen length), from the compressed neutral axis, about 13.5 millimeters (= 67.5 percent of specimen height). Hence the stress distribution must differ substantially from the linear law, according to Navier, in an isotropic bending specimen.

5. IMPACT STRENGTH OF FROZEN WOOD

The breaking strength under impact - determined as ultimate impact energy under the pendulum hammer - in wood is subject to an unusual amount of scattering. Therefore the attainment of somewhat reliable data on the effects of internal or outside influences on the ultimate impact strength of wood calls for the execution of elaborate test series and statistical interpretation; or, the selection of the material must proceed along well-defined rules and the problem itself narrowly restricted. Within the frame-

work of the present research, the second avenue of attack was preferred - that is, laminated-wood specimens with different, but perfectly uniformly distributed moisture content in the hygroscopic state were tested for ultimate impact energy. The results are given in figure 30. At fiber saturation point, the ultimate impact strength is only about 58 percent of that of the kiln-dried state. The scatter was quite small. A further unusual fact is that the ultimate impact strength of laminated wood apparently does not depend upon the freezing temperature; at least, it could not be proved for a test series of 13 specimens of laminated beech wood with an average moisture content of 7.5 percent and cooled at -50° , -40° , -30° , -20° , and -6° . The average ultimate impact strength of the specimens frozen at -50° is 0.690 mkg/cm^2 and 0.684 mkg/cm^2 for those frozen at -6° . On the contrary, Kraemer (reference 31) established a marked temperature effect on synthetic resin products.

From the technical point of view, the ultimate impact strength is probably the most important property, since it affords an insight into the behavior of a substance under dynamic stresses and - as first proved by Monnin (reference 29) - at the same time enables to a certain extent a summary appraisal of its elasticity and static behavior. Intensified research is therefore particularly desirable in this respect, even if the obstacles on wood are great (reference 22). This is dictated not only by the multiplicity of biological and chemical effects acting on the ultimate impact energy of wood - which, in part can cancel, in part intensify, and so bring about the aforementioned fluctuations in spite of careful selection of test specimens - but also by the somewhat coarse test method with the Charpy machine. In the standardized impact test the energy required to break the test specimen is measured (mkg) and referred to the specimen cross section. A more logical way would be to refer the impact energy to the volume of the specimen between the supports. Of course, since the impact energy does not increase in proportion to this volume but manifests a minimum value for a certain slenderness ratio (ratio of span to specimen height), and becomes greater again on shorter as on more slender columns - even this method is unable to accord complete satisfaction (reference 32).

In France, a device for approximate solution of the bearing reaction during impact testing, has been developed.

It consists essentially of a support designed as small Brinell hardness indicator, the pressure of the wood specimen in the impact test acting through a steel ball on an aluminum rod of known hardness. The bearing force is computed from the hardness number and the measured spherical area of indentation. But how the transmission of this force is effectuated, within what time, and whether or not accompanied by oscillations is, of course, impossible to ascertain in this manner. The writer therefore decided on a refined method of ultimate impact testing with the Zeiss piezoelectric indicator. Based on a drawing of the bearing on the pendulum hammer, the Zeiss-Ikon Co. designed a pressure element, on which the bearing reaction acts on the quartz pick-up. A more detailed description of the test set-up and procedure is omitted at this time pending the publication of a detailed report of the new test method and its application to the dynamic testing of wood. The present version should therefore be considered merely as an interim report which, however, even as such, affords a new insight into the processes accompanying the ultimate impact test. The bearing impulses transmitted to a quartz crystal are transformed in electric charges which then, after proper amplification, control a cathode-ray oscillograph. The beam of the oscillograph falls on a strip of optically sensitive paper revolving at high speed. A simultaneously operating chronograph records time marks with 0.001 s distance. Figures 31 to 34 are specimen curves obtained on frozen laminated wood. Fundamentally similar pictures in a large number were obtained for different woods at different moisture contents. They teach the following: The breaking of the wood specimens under the pendulum hammer, at a speed of 4.89 meters per second on contact with the piece, occurs extremely quick. The breaking stress, characterized by the maximum force transmitted to the bearing, was reached within 0.00076 to 0.00113 second on the frozen laminated specimens. Through the striking hammer the bar is excited to vibrations. The first impulse which the hammer imparts to the bar sets up a reaction in the bearings within an extraordinarily short time which, on the average, amounts to about 75 percent of the subsequently highest bearing force reached. The time interval of this first impact is so short that it cannot be measured with the aid of the time marks in the diagrams. But since a propagation of mechanical waves is involved, the duration can be mathematically appraised. The speed of propagation c of the elongation waves in solid bodies follows the equation

$$c = \sqrt{E/\rho} \quad (15)$$

where E is the modulus of elasticity (kg/cm^2) and ρ is the material density ($\text{kg s}^2/\text{cm}^4$). For the explored laminated wood it amounts to

$$E = 168,000 \text{ kg}/\text{cm}^2, \quad \rho = 8.15 \times 10^{-7} \text{ kg s}^2/\text{cm}^4$$

hence $c = 4.5 \times 10^5 \text{ cm/s}$ or $c = 4500 \text{ m/s}$ at the particular temperatures and moisture contents. This speed is equal to the velocity of sound in the laminated wood along the fiber. The pendulum hammer strikes in the middle of the specimen; that is, by a 24-centimeter span to each support the elongation waves have to travel a distance of 12 centimeters. To accomplish this, $\left(\frac{12}{4.5}\right) \times 10^{-5} = 0.0000245$ second are required.

But by virtue of the good elasticity and strength properties of the wood the hammer is by no means able to break the pieces immediately but recoils a little at the first hit. Hammer and test piece form a vibration system. From the point of view of material mechanics, the damping in the wood is significant. Damping is the amount of energy absorbed by the bar itself and obviously is so much greater as the wood is more tenacious. Even though the force-time diagrams recorded with the piezoelectric indicator (without knowing at the same time the vibration amplitudes which, moreover, would have to be plotted by some auxiliary means) afford no absolute data on the damping, they nevertheless give a good comparative picture through the area below the vibration curve up to the breaking stress. The behavior of the bars can be very dissimilar, according to this stress, that is, when the cohesion is largely overcome. By a completely smooth break, a single rapid drop of the pressure on the supports would have to occur. But on wood, it almost always results in splintery and, partially, even long-fibered breaks, so that certain residuary resistances must still be overcome. This appears in the force-time chart as after-vibrations. This is particularly plain on wood which is not split in two by the impact test (such as good ash or hickory). The ratio of energy change before and after breaking might also permit certain deductions.

Translation by J. Vanier,
National Advisory Committee
for Aeronautics.

REFERENCES

1. Tiemann, H. D.: Effect of Moisture upon the Strength and Stiffness of Wood. U.S. Dept. Agric., For. Serv. Bull. No. 70, Washington, D.C., 1906.
2. Baumann, R.: Die bisherigen Ergebnisse der Holzprüfungen in der Materialprüfungsanstalt an der Technischen Hochschule Stuttgart. VDI-Forsch., Heft 231. Berlin: VDI-Verlag 1922, S. 121.
3. Miyai, K., and Oshawa, M.: Experiments in the Bending Strength of Frozen Wood (japanisch geschrieben). Res. Bull. Hokkaido Imperial University, Japan.
4. George, H. D.: The Effect of Low Temperature on the Strength of Wood. Bull. New York State College of Forestry, Syracuse Univ. Tech. Pub. No. 43, Nov. 1933.
5. Vorreiter, L.: Biege- und Druckfestigkeit gefrorenen Holzes. Tharandter Forstl. Jahrb., Bd. 89 (1938), S. 491.
6. Kollmann, F.: Technologie des Holzes. Julius Springer (Berlin), 1936.
7. Kollmann, F.: Vorgänge und Änderungen von Holzeigenschaften beim Dampfen. Holz als Roh- und Werkstoff, Bd. 2 (1939), S. 1.
8. Wilson, T. R. C.: Strength-Moisture Relations for Wood. U.S. Dept. Agric., Tech. Bull. No. 282, Washington, D.C., March 1932, p. 9.
9. Koch, K. R.: Beiträge zur Kenntnis der Elasticität des Eises. Wied. Ann., Bd. 25 (1885), S. 438. Ders.: Über die Elasticität des Eises. Zweite Mitteilung. Ann. Phys. Lpz. (4), Bd. 45 (1914), S. 237.
10. Hess, H.: Elasticität und innere Reibung des Eises. Ann. Phys. Lpz. (4), Bd. 8 (1902), S. 405.
11. Honigmann, E. J. M.: Zur Frage der Frostprobe in der Materialprüfung. Z. ost. Ing.- u. Archit.-Ver., Bd. 84 (1932), S. 64.

12. Sachs, G.: Grundbegriffe der mechanischen Technologie der Metalle. Akad. Verlagsges, Leipzig, 1925.
13. Pillow, M. Y.: Effect of High Temperatures on the Mode of Fracture and Other Properties of a Hardwood. Wood Working Industries, Oct. 1929.
14. Koehler, A., and Pillow, M. Y.: Effect of High Temperatures on the Mode of Fracture and Certain Physical and Mechanical Properties of Sitka Spruce. Southern Lumberman, Dec. 19, 1925.
15. Moräth, E.: Beiträge zur Kenntnis der Quellungserscheinungen des Buchenholzes. Kolloidchem. Beih., Bd. 33 (1931), S. 132.
16. Grüneisen, E.: Zustand der festen Körper (Geiger-Scheel, Handbuch der Physik, Bd. X, S. 48). Julius Springer (Berlin), 1926.
17. Hägglund, E.: Holzchemie, 2. Aufl. Akad. Verlagsges, Leipzig, 1939.
18. Marschallek, B.: Die Einwirkung künstlicher Trocknung bei hohen Temperaturen auf Buchenholz. Mitt. Forstwirtsch. Forstwiss., Bd. 2 (1931), S. 589.
19. Haefeli, R.: Schneemechanik (Bader, Haefeli u.a.) Der Schnee und seine Metamorphose. Beiträge zur Geologie der Schweiz. Geotechnische Serie Hydrologie, Lfg. 3. Elsässer vorm. Müller, Zürich, 1939.
20. Mügge, O.: Über die Plasticität der Eiskristalle. Nachr. kgl. Ges. d. Wiss. Göttingen Math.-phys. Kl. (1895), S. 173.
21. Tiemann, H. D.: The Effect of the Speed of Testing upon the Strength of Wood and the Standardization of Tests for Speed. Proc. Amer. Soc. Test. Mater., vol. 8 (1908), p. 54.
22. Gholmeziu, N.: Untersuchungen über die Schlagfestigkeit von Bauhölzern. Holz als Roh- und Werkstoff, Bd. 1 (1938), S. 585.
23. Meyer, R. H., and Mark, H.: Der Aufbau der hochpolymeren organischen Naturstoffe. Akad. Verlagsges, Leipzig, 1930.

24. Mark, H.: Physik und Chemie der Zellulose. Julius Springer (Berlin), 1932.
25. Holzeigenschaftstafel: Rotbuche. Holz als Roh- und Werkstoff, Bd. 2 (1939), S. 95.
26. Tammann, G.: Über adiabatische Zustandsänderungen eines Systems, bestehend aus einem Kristall und seiner Schmelze. Ann. Phys. Lpz. (4), Bd. 1 (1900), S. 275. Ders: Über das Verhalten des Wassers bei hohen Drucken und tieferen Temperaturen. Z. phys. Chem., Bd. 72 (1910), S. 609. Ders: Kristallisieren und Schmelzen. J. A. Barth, Leipzig, 1903, S. 315.
27. Bridgeman, P. W.: Verhalten des Wassers als Flüssigkeit und in fünf festen Formen unter Druck. Z. anorg. Chem., Bd. 77 (1912), S. 377. Ders: Water, in the Liquid and Five Solid Forms Under Pressure. Proc. Amer. Acad. Arts and Sci., Boston, Bd. 47 (1912), S. 441.
28. Trendelenburg, R.: Das Holz als Rohstoff. J. F. Lehmann, München, 1939.
29. Monnin, M.: Essais physique, statique et dynamique des bois. Bul. Sect. Tech. L'Aeronaut, Paris, June and July 1919. Ders: L'Essais des bois (Kongressbuch Zürich, Int. Verb. Mat.-Prüf., S. 85). Ass. Int. pour l'Essais des Matériaux, Zürich, 1932.
30. Thunell, B.: Temperaturrens inverkan på bojhallfastheten hos svenskt furuvirke. Svenska Skogsvårdsförningens Tidskrift, Bd. 38 (1940), S. 1.
31. Kraemer, O.: Kunstharzstoffe und ihre Entwicklung zum Flugzeugbaustoff (340. DVL-Bericht). DVL Jahrbuch, 1933, S. 74.
32. Kollmann, F.: Über die Schlag- und Dauerfestigkeit der Hölzer (Mitt. Fachaussch. Holzfragen H. 17, S. 17). VDI-Verlag, Berlin, 1937.

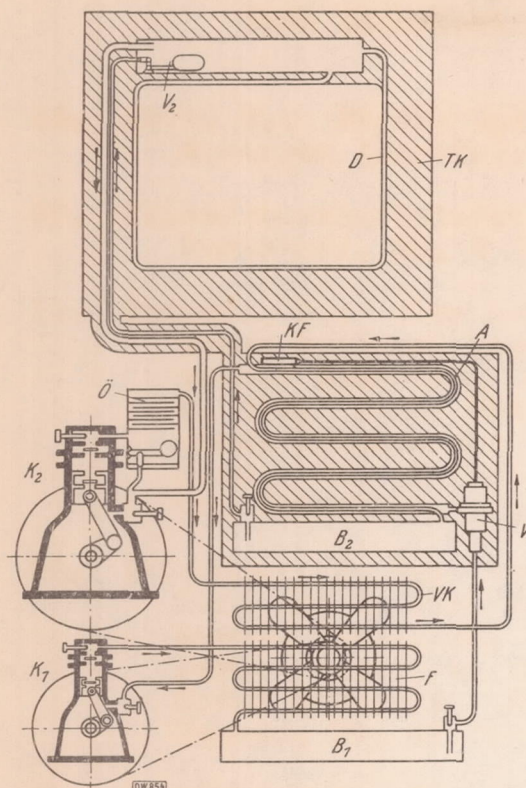


Figure 1.- Low temperature (-60°C) refrigerator-design: Teres
 K_1, K_2 ; Compressor; F, liquifier;
 B_1, B_2 , tank; V_1, V_2 , throttle valve;
 KF, thermostat; O, oil separator;
 VK, precooler; A, heat exchanger;
 D, evaporator; TK, refrigerator.

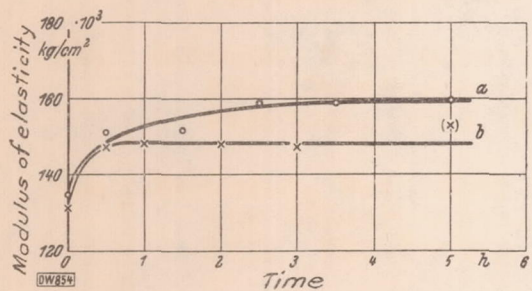


Figure 6.- Rise of elasticity modulus in laminated wood TBu 20 ($u=12\%$) after refrigeration (-50°C). a, sample bare; b, sample in air-tight glass bottle.

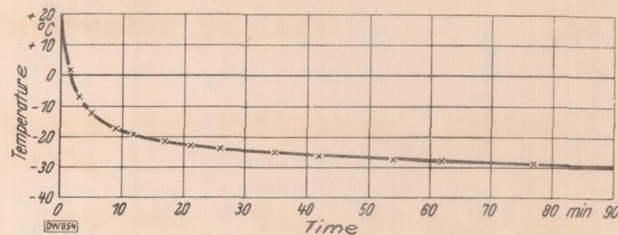


Figure 2.- Temperature variation in a kiln-dried beech block ($2 \times 2 \times 3$ cm) after refrigerator storage (-38°C).

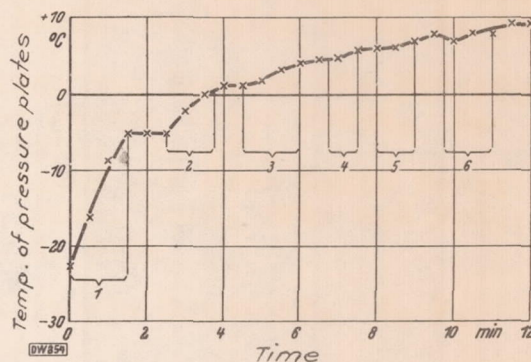


Figure 3.- Temperature of pressure plate of testing machine during a test series.

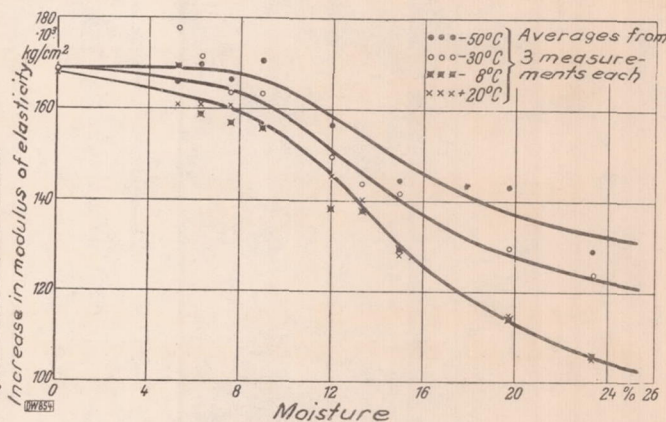


Figure 7.- Elasticity modulus of TBu 20 in the hygroscopic zone at $T = +20^{\circ}$ to -50°C .

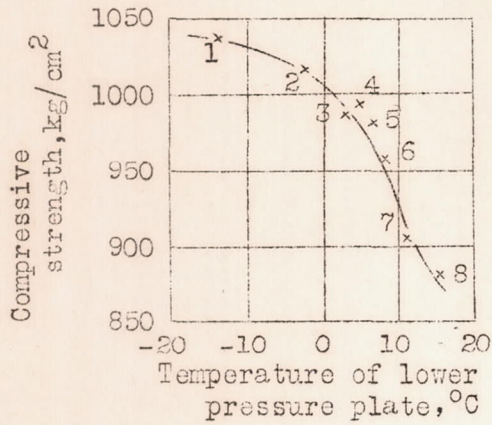


Figure 4.- Decrease of compressive strength of frozen specimens due to heating of pressure plates (of test points 1 to 6 in Fig. 3).

Figure 5.- Deflection of a laminated wood TBu 20 ($u = 7\%$) under average load and for different spans.

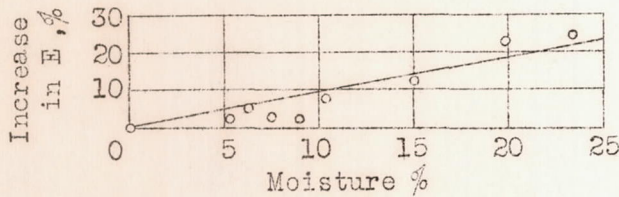
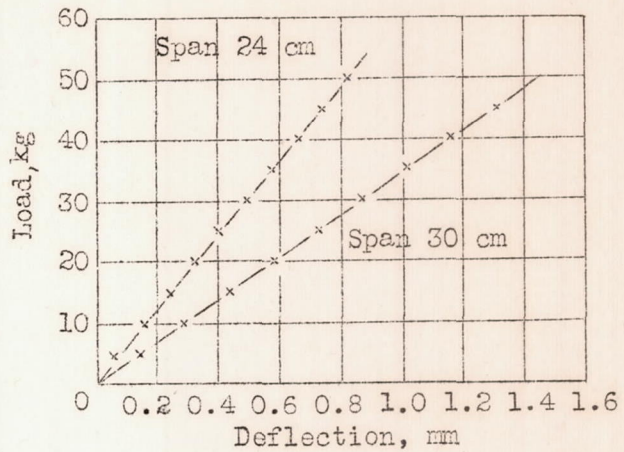
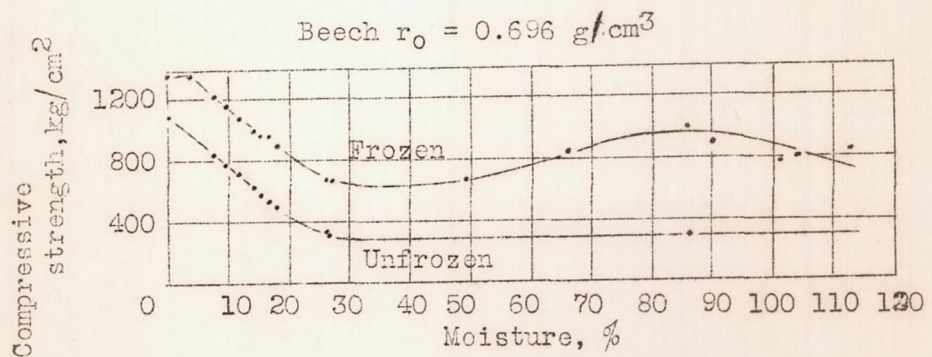


Figure 8.- Proportional rise of elasticity modulus of TBu 20 at -50°C , plotted against room-heated samples of equal moisture content.

Figure 17.- Effect of moisture content on the compressive strength of frozen and unfrozen beech wood.



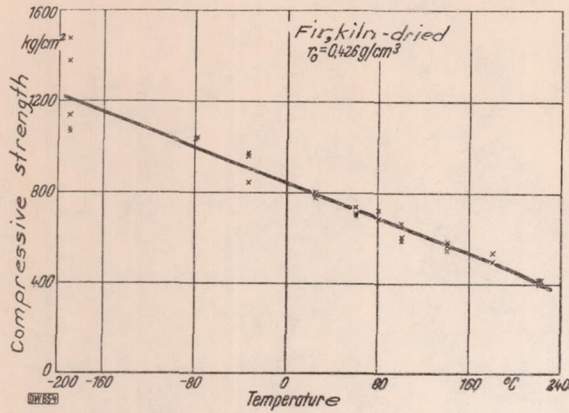


Figure 9.- Effect of temperature on compressive strength of kiln-dried fir.

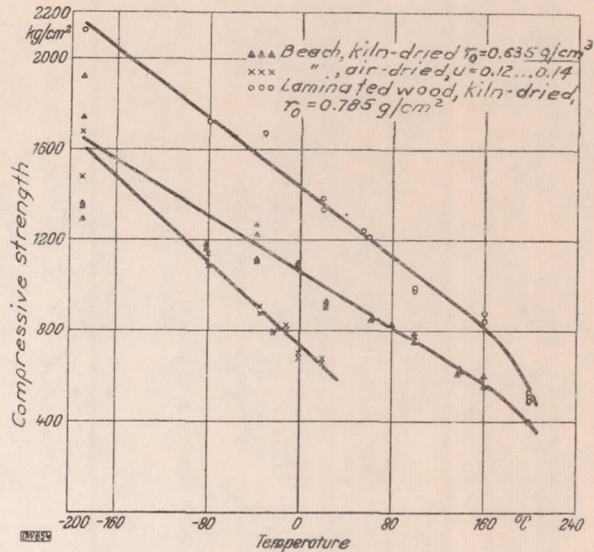


Figure 10.- Effect of temperature on compressive strength of beech, kiln-dried and air-dried, and TBu 20, kiln-dried.

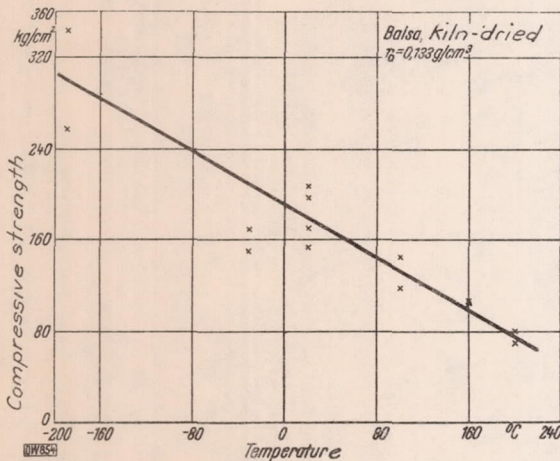


Figure 11.- Effect of temperature on compressive strength of balsa wood, kiln-dried.

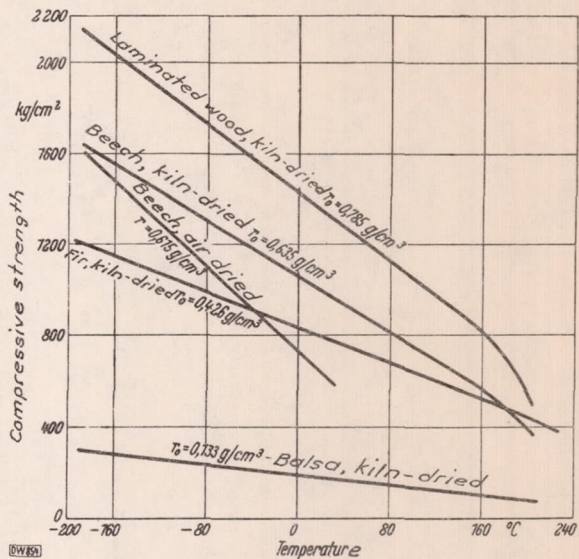


Figure 12.- Effect of temperature on compressive strength of different heavy wood. (Figs. 9 to 11).

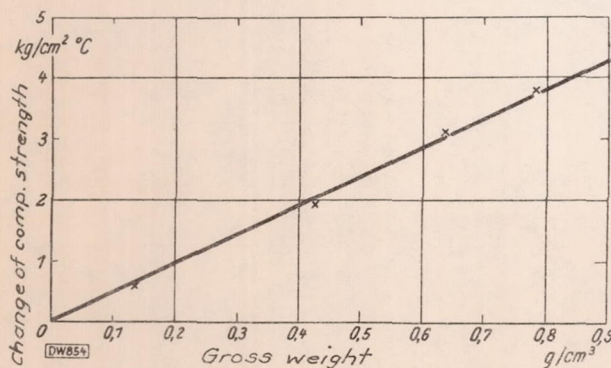
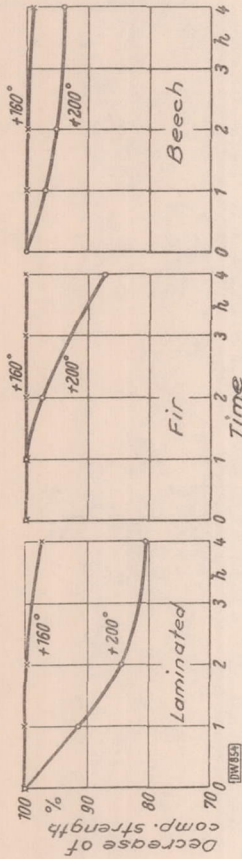
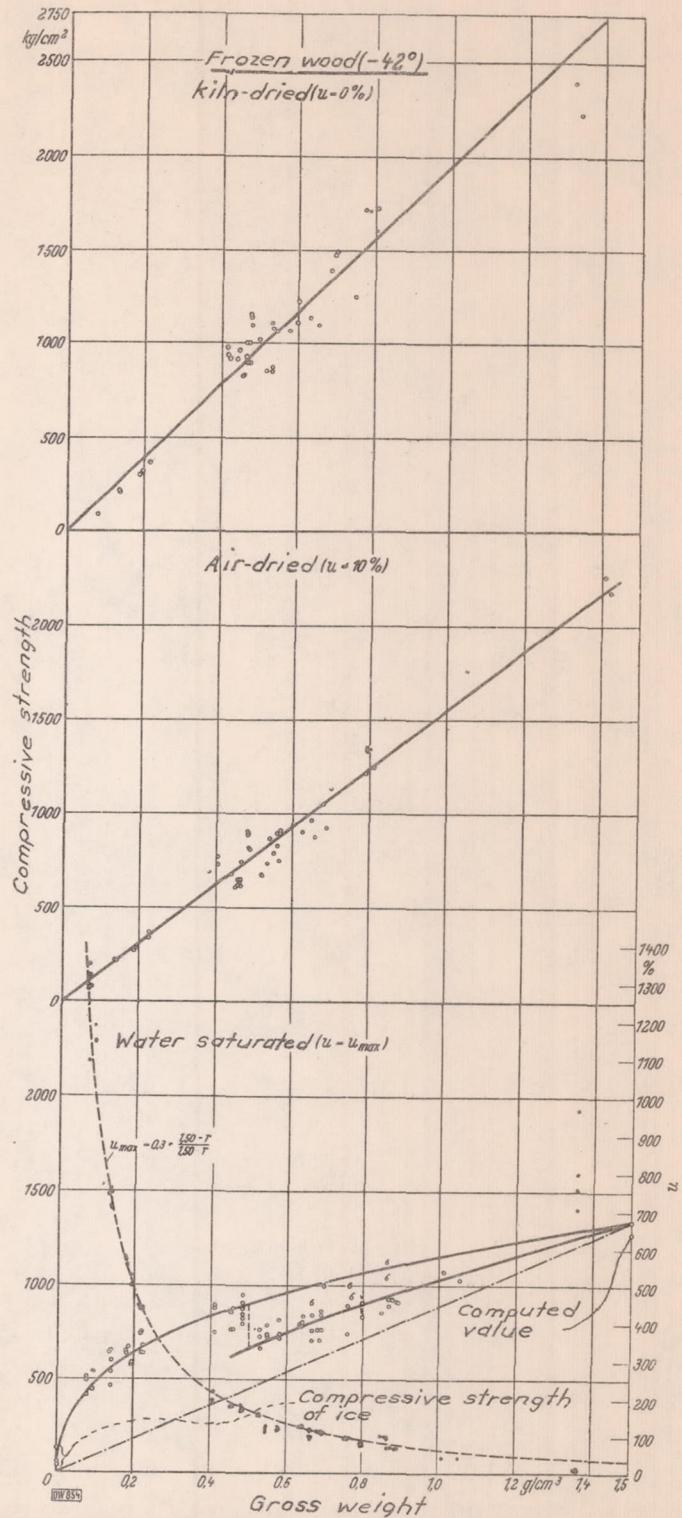


Figure 13.- Ascent of compressive strength-time curves plotted against gross weight. (Figs. 9 to 12).



Figures 14,15,16.- Effect of temperature on compressive strength of laminated wood, fir and beech with respect to time.



Figures 23,24,25.- Relation between gross weight and compressive strength of frozen wood. (-42°C).

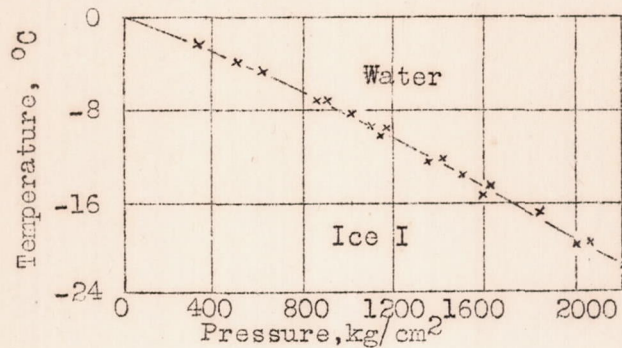


Figure 18.- Limiting curve between strength and crystal phase of water.

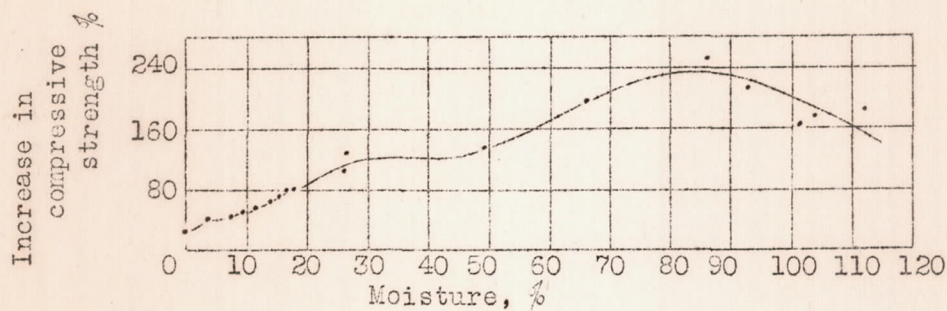


Figure 19.- Rise of compressive strength of frozen beech against nonfrozen samples of the same moisture content.

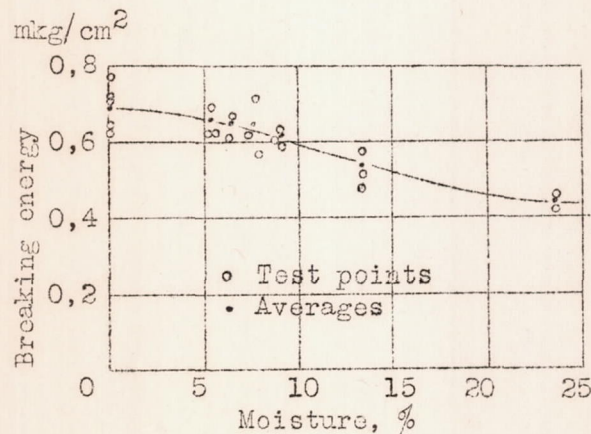
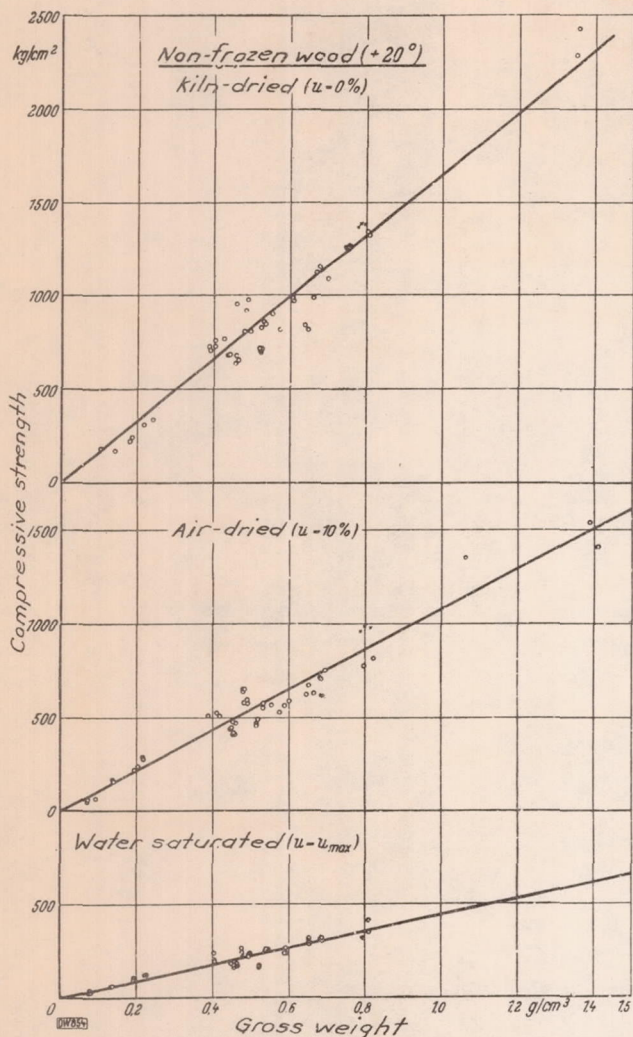


Figure 30.- Breaking energy under impact of frozen laminated wood (-50 °C) in the hygroscopic zone.



Figures 20, 21, 22.- Relations between gross weight and compressive strength of room-heated wood (+20°C).

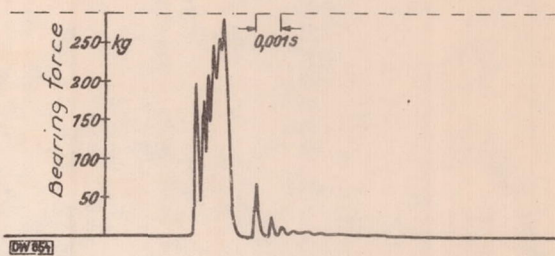


Fig. 31: $t = -60^\circ\text{C}$

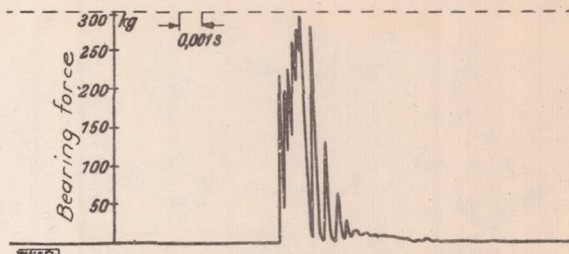


Fig. 32: $t = -50^\circ\text{C}$

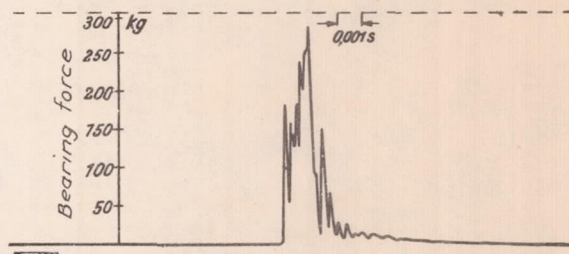


Fig. 33: $t = -40^\circ\text{C}$

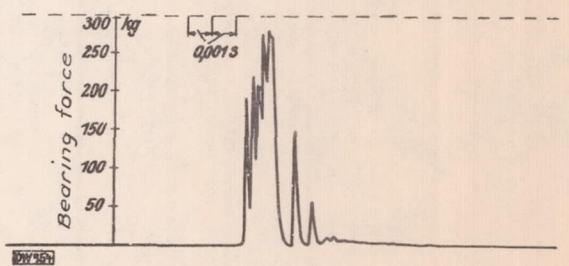


Fig. 34: $t = -20^\circ\text{C}$

Figures 31, 32, 33, 34.- Time rate of fluctuations of the bearing force during the ultimate impact test recorded with Zeiss-Ikon piezo-electric indicator material: laminated TBu 20, $u=6.6\%$.

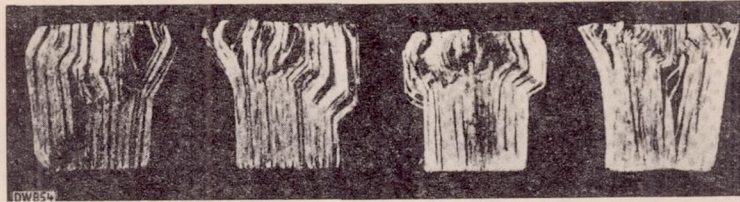


Figure 26.- Break patterns of frozen compression samples of balsa wood. ($u = u_{max}$)

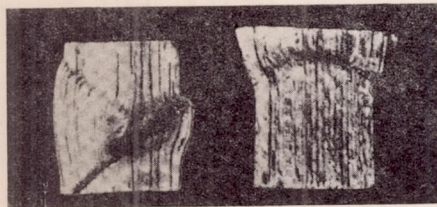


Figure 27.- Break patterns of frozen compression samples of walnut and red beech wood. ($u = u_{max}$)

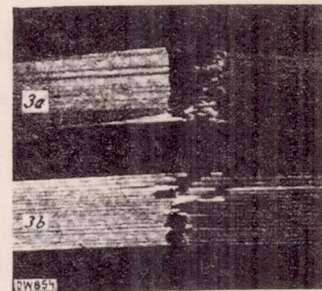


Figure 29.- Bending failure of a frozen (3a) and a room-heated (3b) pine specimen.

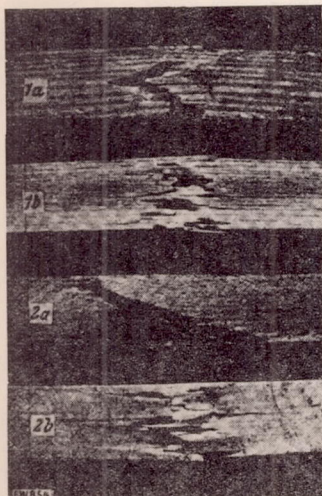


Figure 28.- Break of frozen and room-heated bending specimens.

- 1a, ash frozen
- 1b, ash room-heated
- 2a, beech frozen
- 2b, beech room-heated